*Featured Article*

# Pseudolaric Acid B Inhibits Angiogenesis and Reduces Hypoxia-Inducible Factor 1α by Promoting Proteasome-Mediated Degradation

**Mei-Hong Li,[1,3] Ze-Hong Miao,[1] Wen-Fu Tan,[1] Jian-Min Yue,[2] Chao Zhang,[1] Li-Ping Lin,[1] Xiong-Wen Zhang,[1] and Jian Ding[1]**

[1]Division of Anti-Tumor Pharmacology, State Key Laboratory of Drug Research, and [2]Division of Phytochemistry, Shanghai Institute of Materia Medica, Shanghai Institutes for Biological Sciences, Chinese Academy of Sciences, Shanghai, People's Republic of China [3]Graduate School of the Chinese Academy of Sciences, Beijing, People's Republic of China

## ABSTRACT

***Purpose:*** **Pseudolaric acid B (PAB), the naturally occurring diterpenoid isolated from the root bark of *Pseudolarix kaempferi* Gordon tree (Pinaceae), possesses potent antifungal and pregnancy-terminating effects that may be tightly associated with angiogenesis. This study was to examine its angiogenic inhibition, impact on vascular endothelial growth factor (VEGF) secretion from tumor cells and the possible mechanism of action.**

***Experimental Design:*** **Angiogenesis inhibition was assessed by the human umbilical vascular endothelial cell proliferation, migration, and tube-formation assays, as well as the chorioallantoic membrane assay. ELISA, reverse transcription-PCR, and Western blotting analyses were performed to examine VEGF protein secretion, mRNA expression, and the possible mechanism in hypoxic MDA-MB-468 cells.**

***Results:*** **PAB displayed potent *in vitro* antiangiogenic activity shown by inhibiting VEGF-stimulated proliferation and migration and fetal bovine serum-stimulated tube formation of human umbilical vascular endothelial cells in a concentration-dependent manner. Moreover, PAB (10 nmol per egg) significantly suppressed *in vivo* angiogenesis in the chorioallantoic membrane assay. On the other hand, PAB abrogated hypoxia-induced VEGF secretion from MDA-MB-468 cells via reducing HIF-1α protein. Additional analyses using LY294002 and U0126 indicated that the increase in hypoxia-inducible factor 1 (HIF-1)α protein level was highly dependent on phosphatidylinositol 3′-kinase and p42/p44 mitogen-activated protein kinase activities in hypoxic MDA-MB-468 cells. However, PAB treatment did not affect the active (phosphorylated) forms of Akt and Erk. Interestingly, the selective proteasome inhibitor MG-132 completely reversed the reduction of HIF-1α protein in the PAB-treated MDA-MB-468 cells.**

***Conclusions:*** **PAB displays the dual antiangiogenic activities of directly inhibiting endothelial cells and abrogating paracrine stimulation of VEGF from tumor cells due to reducing HIF-1α protein by promoting its proteasome-mediated degradation in MDA-MB-468 cells, which has potential clinical relevance.**

## INTRODUCTION

Angiogenesis plays a critical role in tumor progression (1, 2). An avascular tumor can rarely increase in size >2–3 $mm^3$. Once vascularized, a tumor grows rapidly and nearly exponentially (2). Moreover, the vascular density of a tumor is closely associated with its metastatic potential and, thus, with its malignancy (3). Therefore, inhibition of tumor angiogenesis has been one of the promising strategies in the development of novel anticancer therapy.

Many growth factors and cytokines are engaged in angiogenesis. Among them, vascular endothelial growth factor (VEGF), which is actively secreted from the neighboring tumor cells (4), is generally regarded as the most potent and specific angiogenic factor (5, 6). It can stimulate endothelial cell proliferation, protease expression, migration, and subsequent differentiation to form new vessels. Enhanced expression of VEGF has been observed in many human cancers, mainly induced by hypoxia under the control of the transcription factor hypoxia-inducible factor 1 (HIF-1; refs. 7–9).

HIF-1, a heterodimer composed of HIF-1α and constitutively expressed HIF-1β subunits, is a basic helix-loop-helix Per-Arnt-Sim transcription factor (10). Its biological activity depends on the amount of HIF-1α, which is tightly regulated by oxygen tension. Under normoxic conditions, HIF-1α is remarkably unstable and is rapidly degraded by the proteasome pathway (11). In contrast, under hypoxic conditions, HIF-1α becomes stable, accumulates, and translocates into the nucleus where it forms an active complex with HIF-1β. This active heterodimer may activate transcription of >40 target genes,

Received 5/14/04; revised 9/15/04; accepted 9/22/04.
**Grant support:** National Natural Science Foundation of China No. 30200345 and No. 30228032.
**Note:** W-F. Tan is currently in the Oral and Pharyngeal Cancer Branch, National Institute of Dental and Craniofacial Research, National Institutes of Health, Bethesda, MD.
The costs of publication of this article were defrayed in part by the payment of page charges. This article must therefore be hereby marked *advertisement* in accordance with 18 U.S.C. Section 1734 solely to indicate this fact.
**Requests for reprints:** Jian Ding, Division of Anti-tumor Pharmacology, State Key Laboratory of Drug Research, Shanghai Institute of Materia Medica, Shanghai Institutes for Biological Sciences, Chinese Academy of Sciences, 555 Zu Chong Zhi Road, Zhangjiang Hi-Tech Park, Shanghai 201203, People's Republic of China. Fax: 86-21-50806722; E-mail: jding@mail.shcnc.ac.cn.

including VEGF, by binding to the DNA consensus sequence 5′-RCGTG-3′ in the promoter regions of those genes (12). However, the regulation of HIF-1 is complex. Besides the proteasome pathway, the phosphatidylinositol 3′-kinase (PI3K) and p42/p44 mitogen-activated protein kinase (MAPK) pathways are also reported to be involved in the regulation of HIF-1 (13, 14). Thus far, it has not been clarified what kind of interrelationship exists between these three pathways in controlling HIF-1α level.

Overexpression of HIF-1α protein has also been demonstrated in human cancers as compared with the respective normal tissues, including colon, breast, gastric, lung, skin, ovarian, pancreatic, prostate, and renal carcinomas (15). A growing body of evidence indicates that HIF-1 contributes to angiogenesis and tumor progression. Tumor xenografts of embryonic stem cells from HIF-1α$^{-/-}$ mice showed decreased growth rate and vascularization relative to the wild-type cells (16). In breast cancer, the HIF-1α level was also closely associated with increased vascularity and tumor progression (17). Therefore, HIF-1 has been considered as a promising target in the antiangiogenesis strategy. To date, however, few angiogenesis inhibitors have been shown to target HIF-1. In this article, we reported that Pseudolaric acid B (PAB; Fig. 1), an active principle of the traditional Chinese medicine known as "Tu-Jin-Pi," inhibited the angiogenesis potential of human endothelial cells and downregulated the level of HIF-1α protein by promoting proteasome-mediated degradation in human tumor cells.

## MATERIALS AND METHODS

**Materials.** PAB was isolated from the ethanolic extract of the root bark of *Pseudolarix kaempferi* by column chromatography and recrystallization, with the purity of 99.3% as determined by high-performance liquid chromatography (18). It was dissolved at a concentration of 0.01 mol/L in 100% DMSO as a stock solution, stored at −20°C, and diluted with sterile water before each experiment. The final DMSO concentration did not exceed 0.1% DMSO throughout the study. LY294002 and U0126 were purchased from Sigma (St. Louis, MO), and MG-132 (Z-Leu-Leu-Leu-CHO) was from Biomol (Plymouth Meeting, PA). Primary antibodies for HIF-1α (sc-10790) and β-actin (sc-1616) were obtained from Santa Cruz Biotechnology (Santa Cruz, CA). Antibodies for p-Akt (#9272), Akt (#9271), p-Erk (#9101), Erk (#9102), were from Cell Signaling Technology (Beverly, MA). Secondary antibodies for horseradish peroxidase-conjugated antirabbit IgG and antigoat IgG were purchased from Calbiochem (San Diego, CA).

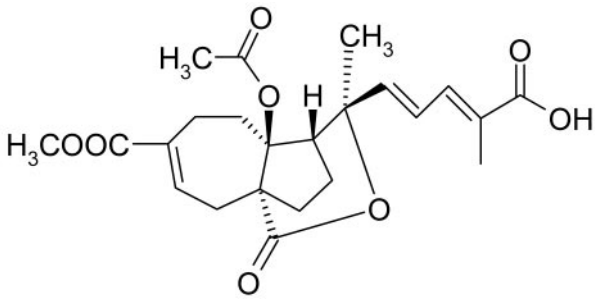


*Fig. 1* Chemical structure of PAB.

**Cell Culture.** Human umbilical vein endothelial cells (HUVECs) were isolated from human umbilical cord veins by 0.1% type-I collagenase digestion at 37°C for 15 minutes and identified by their positive staining for von Willebrand factor antigen (Sigma) using indirect immunofluorescence. HUVECs were grown in M199 medium supplemented with 20% heat-inactivated fetal bovine serum (FBS), 30 μg/mL endothelial cell growth supplement (ECGS; Sigma), 100 units/mL penicillin, and 100 μg/mL streptomycin (Life Technologies, Inc., Grand Island, NY). The cells at three to six passages were used in the experiments.

The human breast cancer MDA-MB-468 and MDA-MB-435 cell lines were obtained from the American Type Culture Collection (Rockville, MD). Cells were cultured in RPMI 1640, supplemented with 10% FBS at 37°C in a humidified atmosphere and 5% $CO_2$ in air (referred to as normoxic conditions). Hypoxia treatment was performed by placing cells in a $CO_2$ Water Jacketed Incubator (Thermo Forma, Model 3110 series), flushed with a mixture of 1% $O_2$, 5% $CO_2$, and 94% nitrogen.

**Influence of PAB on MDA-MB-468 Tumor Cells.** MDA-MB-468 cells ($7.5 \times 10^3$ cells per well for 72-hour assay and $3 \times 10^4$ cells per well for 16-hour assay) were seeded to 96-well plates in RPMI 1640 containing 10% FBS for attachment overnight. Then the cells were treated with different concentrations of PAB for 72 hours and 16 hours, respectively. The number of cells was estimated by the Sulforhodamine B (Sigma) assay. Briefly, after being fixed with 10% trichloroacetic acid at 4°C for 1 hour, the cells were stained with 100 μL per well Sulforhodamine B solution [0.4% Sulforhodamine B (w/v) in 1% acetic acid (v/v)] at room temperature for 15 minutes and washed with 1% acetic acid to remove any unbound dye. Bound dye was solubilized with 10 mmol/L Tris base (pH 10.5). The absorbance values of the plates were measured using a multiwell spectrophotometer (VERSAmax, Molecular Devices, Sunnyvale, CA) at a wavelength of 515 nm (19), and the inhibition rate was calculated by the formula: inhibition rate of proliferation (%) = $(A_{control} - A_{PAB})/A_{control} \times 100\%$. The $IC_{50}$ was fitted with 4-parameter curve. The data were expressed as mean ± SD from three independent experiments.

**VEGF-Stimulated Cell Proliferation Assay.** HUVECs ($5 \times 10^3$ cells per well) were seeded to 96-well plates in M199 medium containing 20% FBS for attachment overnight. Then they were starved in M199 medium containing 1% FBS for 24 hours. After being washed with PBS three times, the cells in fresh medium containing 1% FBS were preincubated with different concentrations of PAB for 1 hour before the addition of 20 ng/mL VEGF. After incubation for 72 hours, the number of cells was estimated by the Sulforhodamine B assay, and the inhibitory effect of PAB on VEGF-stimulated cell proliferation was expressed as the relative value using the formula $A_{treated}/A_{non\text{-}VEGF\ stimulated}$, whereas the relative value of the non-VEGF–stimulated group was defined as 1.

**VEGF-Stimulated Cell Migration Assay.** HUVEC migration assay was performed in a transwell Boyden Chamber (Costar, MA) using a polycarbonate filter with a pore size of 8 μm (20), which was coated with 1% gelatin. In the standard assay, 0.1 mL of cell suspension ($5 \times 10^5$ cells/mL) with PAB

or control [0.05% DMSO (v/v)] diluted in serum-free M199 medium was added to the upper compartment of the chamber. The lower compartment contained 0.6 mL of serum-free M199 medium supplemented with 10 ng/mL VEGF. After a 6-hour incubation at 37°C, all of the nonmigrant cells were removed from the upper face of the transwell membrane with a cotton swab; the migrated cells were fixed with 90% EtOH and then stained with 0.1% crystal violet in 0.1 mol/L borate and 2% EtOH (pH 9.0). The stained cells were subsequently extracted with 10% acetic acid. The absorbance values were determined at 600 nm (21), and the inhibition rate of migration was calculated using the formula: inhibition rate of migration = $[1 - (A_{PAB} - A_{blank})/(A_{control} - A_{blank})] \times 100\%$.

**Tube Formation Assay.** Tube formation of HUVECs was conducted for the assay of *in vitro* angiogenesis (22). Briefly, a 96-well plate was coated with 50 μL of Matrigel (Becton Dickinson Labware, Bedford, MA), which was allowed to solidify at 37°C for 1 hour. HUVECs ($1 \times 10^4$ cells per well) were seeded on the Matrigel and cultured in M199 medium containing different concentrations of PAB or control [0.05% DMSO (v/v)] for 8 hours. The enclosed networks of complete tubes from five randomly chosen fields were counted and photographed under a microscope (IX70, Olympus, Tokyo, Japan). The inhibition rate was calculated using the following formula: Inhibition rate of tube formation = $[1 - (\text{tubes}_{PAB}/\text{tubes}_{control})] \times 100\%$.

**Chicken Chorioallantoic Membrane (CAM) Assay.** Inhibition of angiogenesis *in vivo* was measured using a modified CAM assay (23). Fertilized chicken eggs were incubated in a humidified egg incubator Roll-X base (Lyon Electric Company, Chula Vista, CA) for 9 days. After this incubation, a small hole was punched on the broad side of the egg, and a window was carefully created through the egg shell directly over embryonic blood vessels, which was determined by candling before the experiment. Filter paper disks saturated with PAB (2, 10, and 50 nmol/10 μL per egg) or control [0.05% DMSO (v/v)] were placed on the CAMs. The eggs were then returned to the humidified egg incubator for 2 days of incubation, after which time CAMs were scissored off and fixed in 4% paraformaldehyde for 15 minutes. The vessels were photographed using a microscope (BX51 Olympus) at a magnification of ×40. Angiogenesis was quantified by counting the vessel branch points on CAMs. The inhibition rate of angiogenesis was calculated using the following formula: Inhibition rate of angiogenesis = $[1 - (\text{vessel branch points})_{PAB}/(\text{vessel branch points})_{control}] \times 100\%$. Ten eggs were tested for each group, and the assay was performed twice to ensure reproducibility.

**Conditioned Medium and ELISA for VEGF.** MDA-MB-468 cells were seeded in a six-well plate at a density of $5 \times 10^5$ cells per well in RPMI 1640 supplemented with 10% FBS. After attachment, the medium was replaced with 1 mL per well of fresh medium, and the cells were treated with PAB (0.313, 0.625, 1.25, and 2.5 μmol/L) or vehicle [0.025% DMSO (v/v)], and then subjected to hypoxia or normoxia for 16 hours as described in the "Cell Culture" section. Cell supernatants were collected, clarified by centrifugation at 300 × *g* for 5 minutes, and stored at −20°C. Simultaneously, cell pellets were harvested by trypsinization, and cell number was determined by the trypan blue dye exclusion test. The amount of VEGF in the supernatant was determined with a VEGF-ELISA kit (R&D Systems, Minneapolis, MN) according to the manufacturer's instructions. VEGF was expressed as picograms of VEGF protein per milliliter of medium and per $10^5$ cells (24).

**Semiquantitative Reverse Transcription-PCR.** After treatment of MDA-MB-468 cells ($5 \times 10^5$ cells per well) with PAB or vehicle [0.025% DMSO (v/v)] under hypoxia or normoxia for 6 hours as described in the "Cell Culture" section, total RNA was isolated using Trizol reagent (BBI, Toronto, Ontario, Canada) according to the manufacturer's instructions. RNA yield and purity was assessed by spectrophotometric analysis. Total RNA (1 μg) from each sample was subjected to reverse transcription with random hexamer, deoxynucleoside triphosphates, and Moloney murine leukemia virus reverse transcriptase in a total reaction volume of 20 μL. PCR was performed on cDNA with the use of *Taq*DNA polymerase, deoxynucleoside triphosphates, and the corresponding primers. The following PCR primers synthesized by the Shanghai Research Center of Biotechnology, Chinese Academy of Sciences, were used: 5′-TCG GGC CTC CGA AAC CAT G-3′ (sense) and 5′-CCT GGA GAG AGA TCT GGT TC-3′ (antisense) for the *VEGF* gene (25); 5′-CCC CAG ATT CAG GAT CAG ACA-3′ (sense) and 5′-CCA TCA TGT TCC ATT TTT CGC-3′ (antisense) for the *HIF-1*α gene (26); and 5′-CCA TGG AGA AGG CTG GGG-3′ (sense) and 5′-CAA AGT TGT CAT GGA TGA CC-3′ (antisense) for the *GAPDH* gene (27). An aliquot of each reaction mixture was analyzed by electrophoresis on a 2% agarose gel. After being stained with ethidium bromide, the gel images were obtained using GeneSnap Version 6.00 software (Syngene, Cambridge, England), and densitometric analysis was performed using GeneTools Analysis Software Version 3.02.00 (Syngene).

**Western Blotting Analysis.** The tested tumor cells ($5 \times 10^5$ cells per well) were exposed to different concentrations of PAB and/or other reagents for the indicated times, under hypoxic or normoxic conditions as described in the "Cell Culture" section. After removal of the supernatants, the cells were lysed in 1 × SDS gel loading buffer [50 mmol/L Tris-HCl (pH6.8), 100 mmol/L DTT, 2% SDS, 0.1% bromphenol blue, and 10%

*Table 1* Influence of PAB on MDA-MB-468 tumor cells for 72 hours and 16 hours

| Inhibition rate (%) | PAB(μM) | | | | | | | | $IC_{50}$ (μM) |
|---|---|---|---|---|---|---|---|---|---|
| Treatment time | 0.156 | 0.313 | 0.625 | 1.25 | 2.5 | 5 | 10 | 20 | |
| 72 hours | 4.76 ± 0.84 | 24.11 ± 4.83 | 73.64 ± 0.88 | 76.11 ± 1.85 | 77.89 ± 1.05 | 79.19 ± 1.13 | 81.79 ± 2.64 | 83.41 ± 2.40 | 0.42 ± 0.01 |
| 16 hours | 2.42 ± 1.14 | 1.33 ± 1.45 | 6.34 ± 0.96 | 10.20 ± 3.98 | 11.97 ± 2.54 | 10.76 ± 1.62 | 12.10 ± 0.84 | 14.22 ± 2.38 | - |

NOTE. The data were expressed as mean ±SD from three independent experiments.

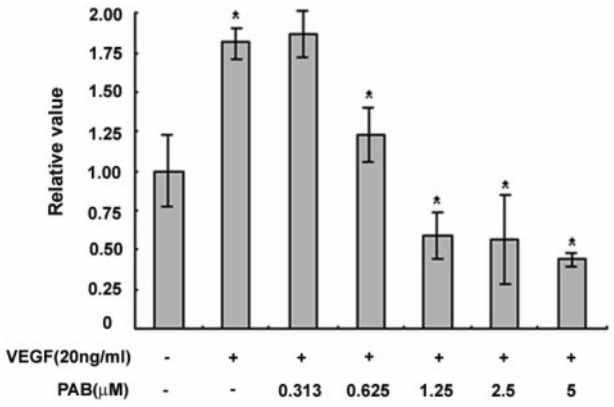


*Fig. 2* Effect of PAB on VEGF-stimulated HUVECs proliferation. Cells were treated with 0.313 to 5 μmol/L PAB in the presence of 20 ng/mL VEGF for 72 hours, and growth inhibition was measured as described in Materials and Methods and expressed as the relative value using the formula $A_{treated}/A_{non\text{-}VEGF\ stimulated,}$ whereas the relative value of the non-VEGF stimulated group was defined as 1. Values are expressed as mean from three separate experiments. $*P < 0.05$, VEGF (+) *versus* VEGF(−), PAB treatments *versus* VEGF (+); *bars,* ±SD.

glycerol] and then boiled for 5 to 10 minutes. Samples with equal amount of cell lysates were loaded and separated on 10% SDS polyacrylamide gels. Proteins on gel were then electrotransferred to Hybond-C nitrocellulose membranes and incubated with the indicated primary antibodies, followed by incubation with horseradish peroxidase-conjugated secondary antibodies. Immunoreactivity was visualized by exposure to X-ray film using SuperSignal West Pico Chemiluminescent Substrate (Pierce, Inc., Rockford, IL) according to the manufacturer's instructions.

## RESULTS

**PAB Inhibits MDA-MB-468 and VEGF-Stimulated HUVEC Proliferation.** PAB has been indicated to possess prominent growth inhibition against tumor cell lines (28). To define its experimental concentration range in the following studies, we examined the effects of PAB on MDA-MB-468 cells and VEGF-stimulated HUVEC proliferation using the Sulforhodamine B assay. Although PAB displayed significant cytotoxicity against MDA-MB-468 tumor cells with an $IC_{50}$ of 0.42 μmol/L for 72-hour treatment, it was little cytotoxic when the duration of treatment was shortened to 16 hours. PAB treatment at a high concentration of 20 μmol/L for 16 hours led to merely 14.22% inhibition on MDA-MB-468 cells (Table 1). On the other hand, VEGF significantly stimulated HUVECs proliferation under the condition of low serum. The number of endothelial cells incubated with VEGF (20 ng/mL) in 1% FBS containing medium for 72 hours increased by 1.81-fold as compared with the control cells grown in 1% FBS containing medium without VEGF. With an $IC_{50}$ of 0.81 μmol/L, PAB reduced the number of HUVECs incubated with VEGF in a concentration-dependent manner to levels below that of the control cells incubated without VEGF (Fig. 2). This demonstrated that PAB could obviously inhibit VEGF-stimulated HUVEC prolifera-

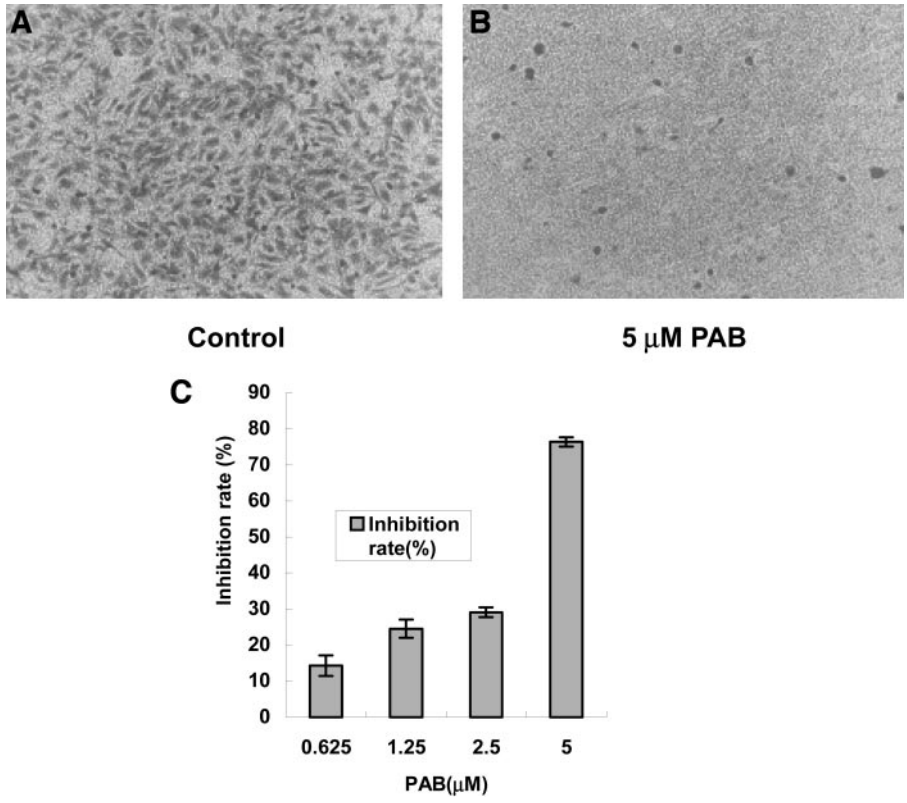


*Fig. 3* Effect of PAB on VEGF-stimulated HUVECs migration. HUVECs ($5 \times 10^4$ cells) suspended in serum-free M199 medium with 0.625 to 5 μmol/L PAB were placed into a transwell and stimulated with 10 ng/mL VEGF. After incubation for 6 hours at 37°C, the migrant cells were photographed and quantified as described in Materials and Methods. *A,* control, 0.05% DMSO. *B,* treatment with 5 μmol/L PAB. Magnification: ×100. *C,* inhibition rate of HUVECs migration by PAB. Values are expressed as mean; *bars,* ±SD, $n = 3$.

tion. In the following studies, all of the functional assays were performed using optimal subcytotoxic concentrations of PAB.

**PAB Reduces VEGF-Stimulated HUVEC Migration.** Endothelial cell migration is a prerequisite for angiogenesis. VEGF is a potent stimulator for the migration of endothelial cell (5). We determined the effect of PAB on *in vitro* HUVEC migration stimulated with VEGF using the Boyden chamber assay. After stimulating HUVECs with VEGF (10 ng/mL) for 6 hours, a large number of them migrated to the lower side of the filter in the Boyden Chamber (Fig. 3*A*), whereas few control cells (without VEGF) were found in the lower chamber. PAB treatment at the concentrations of 0.625 to 5 μmol/L significantly reduced the number of migrated cells in a concentration-dependent manner, with an $IC_{50}$ value of 2.92 μmol/L (Fig. 3*B* and *C*). No cytotoxicity against HUVECs was observed under the same concentrations of PAB for 6 hours used in the above experiment.

**PAB Suppresses Tube Formation of HUVECs.** We next evaluated the effect of PAB on the formation of functional tubes by HUVECs plated on the Matrigel, a reconstituted extracellular matrix preparation of the Englebreth-Holm-Swarm mouse sarcoma. Serum was used as the stimulator in this study, because previous reports (29) and our pretests indicated that VEGF failed to induce tube formation. In the control group stimulated with 20% FBS, HUVECs rapidly aligned with one another and formed tube-like structures resembling a capillary plexus within 8 hours, which required cell-matrix interaction, intercellular communication, as well as cell motility (Fig. 4*A*). PAB prevented FBS-stimulated tube formation of HUVECs in a concentration-dependent manner, with an $IC_{50}$ value of 2.60 μmol/L for 8 hours (Fig. 4*B* and *C*). Meanwhile, no cytotoxicity was observed under this concentration range of PAB. Therefore, PAB was revealed to interfere with the ability of HUVECs to form the *in vitro* vessel-like tube, one of the important traits of the cells.

**PAB Reduces Neovascularization of the CAM.** The CAM of the chicken embryo provides a unique model for investigating the process of new blood vessel formation and vessel responses to antiangiogenic agents. Using this model, we additionally examined the potential *in vivo* antiangiogenic activity of PAB. New blood vessels formed well on CAMs in the control group (Fig. 5*A*). PAB treatment at 2 nmol per egg for 48 hours showed a notable inhibition (Fig. 5*B*), whereas 10 nmol per egg PAB drastically lowered neovascularization of the CAM, accompanied by a lack of prominent vessel networks (Fig. 5*C*). Up to 50 nmol PAB per egg, the inhibition was getting more prominent (Fig. 5*D* and *E*). The data validated the *in vitro* antiangiogenic effectiveness of PAB.

**PAB Abrogates Hypoxia-Induced VEGF Secretion from MDA-MB-468 Cells.** Our current results indicate the antiangiogenic activity of PAB. It has been shown that VEGF, actively secreted from hypoxic tumor cells, could potently trigger tumor angiogenesis. Reduction of VEGF will weaken its stimulation for tumor angiogenesis (5). We additionally examined the effect of PAB on VEGF secretion from the hypoxic MDA-MB-468 cells. The ELISA analysis showed that hypoxia

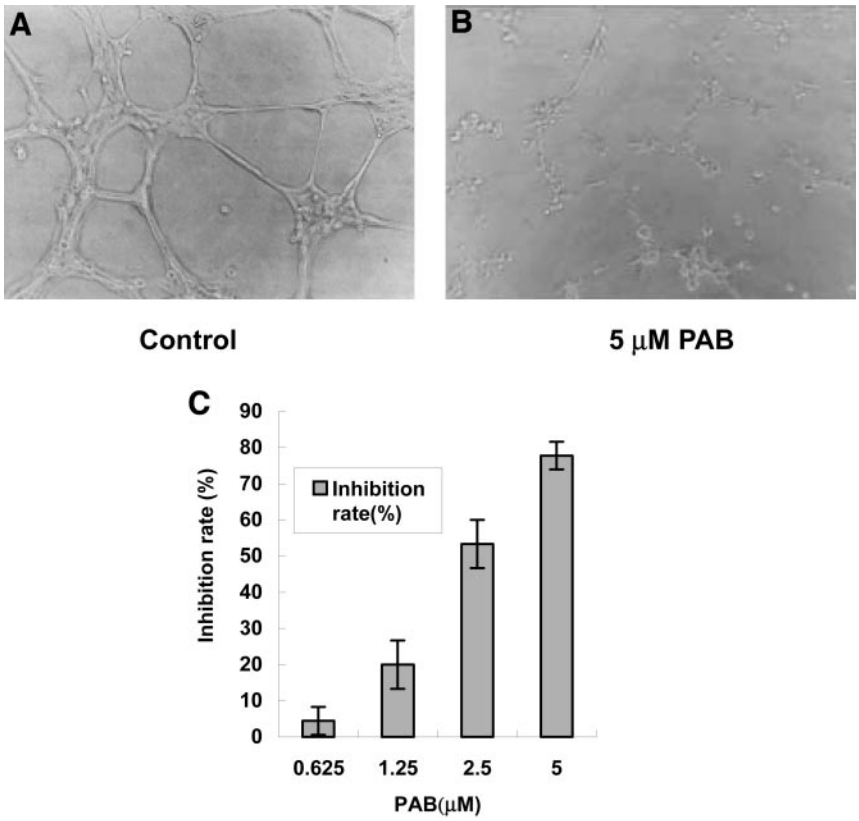


*Fig. 4* Effect of PAB on HUVECs tube formation. HUVECs ($1 \times 10^4$ cells) suspended in M199 medium with 0.625 to 5 μmol/L PAB were added to the Matrigel. After incubation for 8 hours at 37°C, capillary networks were photographed and quantified. *A,* control, 0.05% DMSO. *B,* treatment with 5 μmol/L PAB. Magnification: ×100. *C,* inhibition rate of HUVECs tube formation by PAB. Values are expressed as mean; *bars,* ±SD, $n = 3$.

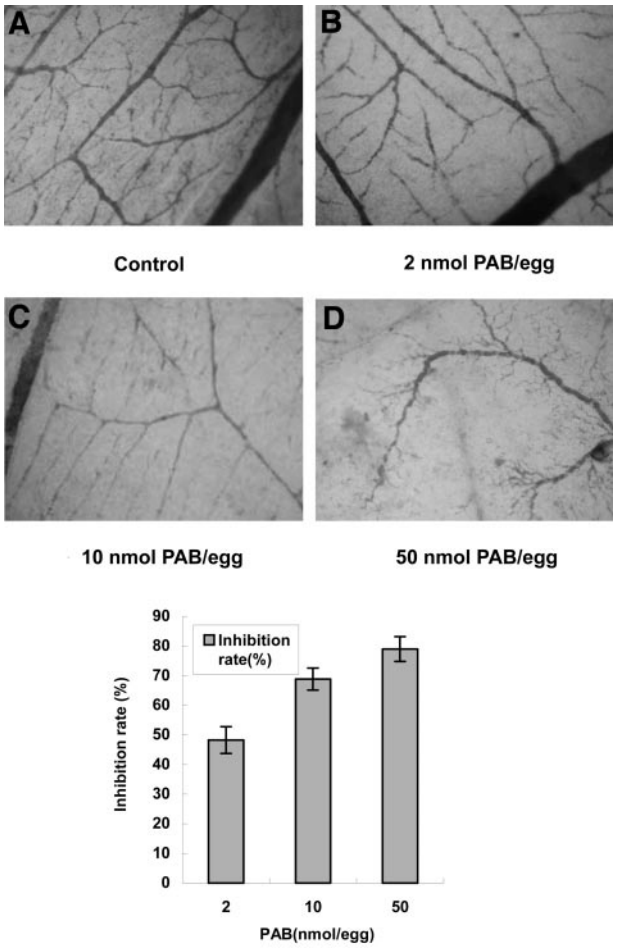


*Fig. 5* Effect of PAB on CAM assay. After fertilized chicken eggs were incubated for 9 days, filter paper disks saturated with PAB (2 to 50 nmol/10 μL per egg) or 0.05% DMSO in double-distilled $H_2O$ (v/v) were placed on the CAMs. Two days later, CAMs were scissored off, fixed, and photographed. *A,* control, 0.05% DMSO. *B,* 2 nmol PAB per egg. *C,* 10 nmol PAB per egg. *D,* 50 nmol PAB per egg. Magnification: ×40. *E,* inhibition rate of angiogenesis on CAMs by PAB. Values were expressed as mean; *bars,* ±SD, $n = 2$.

treatment for 16 hours induced a 1.94-fold increase in VEGF secretion relative to the baseline level. PAB, in a concentration-dependent manner, decreased the VEGF levels in the medium of hypoxic MDA-MB-468 cells. At a concentration of 2.5 μmol/L, PAB almost completely abrogated a hypoxia-induced VEGF rise (Fig. 6). At the same time, cell viability, as determined by the trypan blue dye exclusion test, was not significantly affected by the PAB treatment.

The abrogation of hypoxia-induced VEGF secretion may result from reduced VEGF production in the hypoxia-treated MDA-MB-468 cells. Therefore, we measured the VEGF mRNA expression in hypoxic MDA-MB-468 cells incubated with or without PAB. VEGF mRNA expression sharply increased in hypoxia-treated MDA-MB 468 cells, and PAB treatment decreased its expression in a concentration-dependent manner, which was in accordance with the change of its protein secretion from the cells (Fig. 7*A* and *B*).

**PAB Does Not Affect the Transcription But Lowers the Protein Level of HIF-1α.** Transcription of VEGF gene is tightly regulated by the level of HIF-1α in hypoxic tumor cells. Thus, we examined the level of HIF-1α expression in the PAB-treated cells using reverse transcription-PCR and Western blotting analysis. Neither hypoxia nor PAB plus hypoxia evidently changed the level of HIF-1α mRNA in MDA-MB 468 cells (Fig. 7*A* and *B*). The level of HIF-1α protein was, however, greatly increased by hypoxia and was reduced by PAB, in a concentration-dependent manner. The level of HIF-1α protein began to decrease at 1.25 μmol/L of PAB, and disappeared almost completely at 10 μmol/L (Fig. 8*A*). To validate this result, we additionally examined the effect of 10 μmol/L PAB on the level of HIF-1α protein in another breast tumor cell line, MDA-MB-435. PAB displayed the similar HIF-1α inhibition in this cell line (Fig. 8*B*). The results suggest that PAB may down-regulate the level of HIF-1α protein via accelerating its degradation in this system.

**Inhibition of HIF-1α by PAB Is Not Mediated by PI3K and p42/p44 MAPK Pathways.** To determine whether PI3K and p42/p44 MAPK pathways were involved in the reduction of HIF-1α protein induced by PAB, we first exposed MDA-MB-468 cells to LY294002 (PI3K inhibitor) or U0126 (MEK inhibitor) under hypoxic conditions. The hypoxia-induced rise of HIF-1α protein was reversed markedly by 50 μmol/L LY294002 or 100 μmol/L U0126, indicating that the increase in HIF-1α protein level was highly dependent on PI3K and p42/p44 MAPK activities in hypoxia-treated MDA-MB-468 cells (Fig. 9*A*). Akt and Erk are the vital components in the PI3K pathway and the p42/p44 MAPK pathway, respectively. However, PAB treatment did not affect their active (phosphorylated) forms (Fig. 9*B*), which suggested that the down-regulation of HIF-1α protein level by PAB might be irrelevant to these two pathways in hypoxia-treated MDA-MB-468 cells.

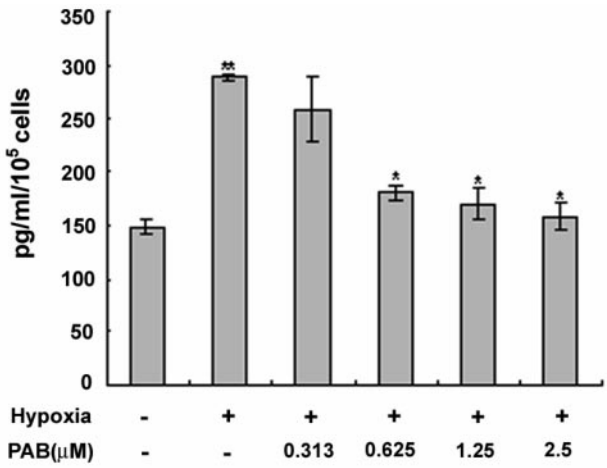


*Fig. 6* Effect of PAB on hypoxia-induced VEGF secretion in MDA-MB-468 cells. Cells were cultured under hypoxia for 16 hours in the presence of concentrations of PAB as indicated, and supernatants were assayed for VEGF content by ELISA. Cell number was determined by the trypan blue dye exclusion test, and the amount of secreted VEGF protein was expressed as pg/mL per $10^5$ cells. Values are expressed as mean; *bars,* ±SD. $n = 3$. *, $P < 0.05$, **, $P < 0.01$, hypoxia (+) *versus* hypoxia (−), PAB treatments *versus* hypoxia (+).

**PAB Accelerates HIF-1α Protein Degradation via the Proteasome Pathway.** Degradation of HIF-1α protein occurs mainly via the ubiquitin-proteasome system (30). We additionally examined whether PAB accelerates HIF-1α protein degradation via the proteasome pathway using the selective proteasome inhibitor MG-132 (31). Alone, MG-132 was able to induce the accumulation of HIF-1α protein, whereas PAB alone resulted in its decrease. Interestingly, complete prevention from degradation was observed when the cells were simultaneously treated with both MG-132 and PAB, irrespective of whether it is under normoxic or hypoxic conditions (Fig. 10). The result strongly suggests that PAB might promote the activity of the proteasome system and, thus, accelerate HIF-1α protein degradation.

## DISCUSSION

PAB is a diterpenoid isolated from the root bark of Pseudolarix kaempferi Gordon tree (Pinaceae). Previous findings indicate that it possesses potent antifungal and cytotoxic activities as well as pregnancy-terminating effects (28, 32), in which angiogenesis is involved. In this study, we first demonstrated the antiangiogenic ability of PAB by effectively suppressing *in vitro* proliferation, migration, and tube formation of HUVECs. Moreover, the CAM assay, in which PAB repressed the *in vivo* angiogenesis, validated the *in vitro* results. Additionally, another study in our laboratory discovered that the inhibition of PAB on tubulin polymerization in endothelial cells was distinct from other known tubulin inhibitors such as colchicine, vincristine, and taxol.[4] These results indicate that PAB can directly inhibit the angiogenesis potential of human endothelial cells.

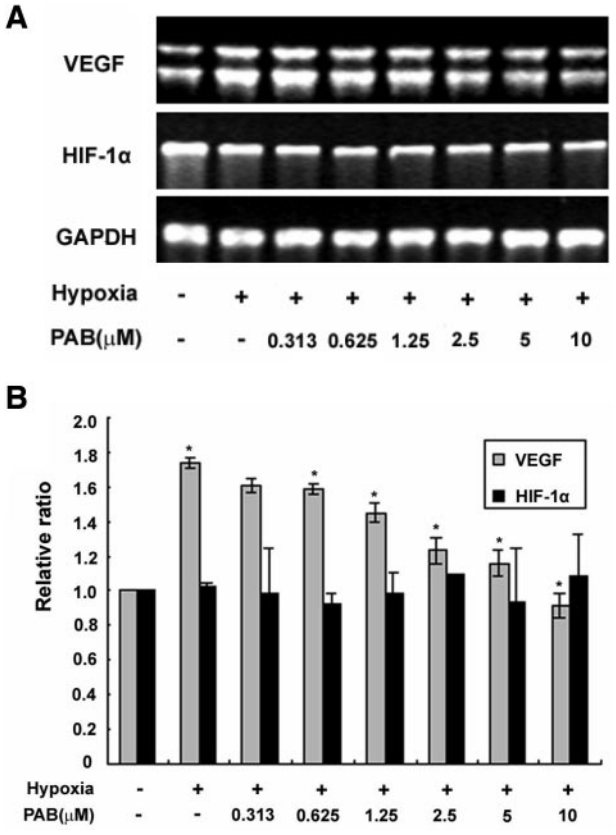


*Fig. 7* Effect of PAB on the transcriptional level of HIF-1α and VEGF genes in MDA-MB-468 cells. mRNAs for *VEGF, HIF-1α,* and *GAPDH* genes were isolated from the MAD-MB-468 cells treated with the indicated concentrations of PAB and cultured under hypoxia for 6 hours. mRNA expression was analyzed by semiquantitative reverse transcription-PCR. *A,* results of reverse transcription-PCR analysis. *B,* semiquantitation of HIF-1α and VEGF cDNA shown in *A* by densitometric analysis. Relative ratio represented the intensities of *HIF-1α* or *VEGF* gene expression relative to those of *GAPDH* expression, whereas the relative ratio in normoxia control was defined as 1. Data were expressed as mean; *bars,* ±SD, $n = 3$. ∗, $P < 0.05$, hypoxia (+) *versus* hypoxia (−), PAB treatments *versus* hypoxia (+).

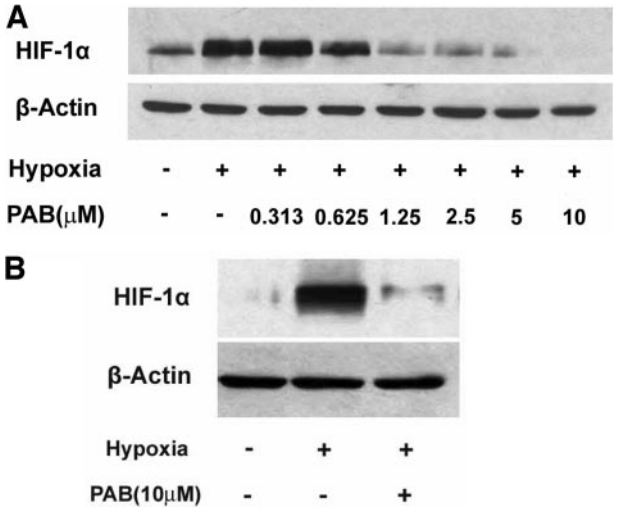


*Fig. 8* Effects of PAB on the levels of HIF-1α protein in tumor cell lines. MDA-MB-468 cells (*A*) and MDA-MB-435 cells (*B*) were treated with the indicated concentrations of PAB under hypoxia for 16 hours. Then, the cells were lysed and detected with HIF-1α and β-actin antibodies by Western blotting. Data shown were representative of three independent experiments.

Interestingly, we have additionally found that PAB could also reduce the stimulator VEGF secretion and its corresponding mRNA level in hypoxic human breast tumor MDA-MB-468 cells (Figs. 6 and 7). Simultaneously, PAB potently decreased HIF-1α protein, although it did not alter HIF-1α mRNA expression in these low-oxygenated cells. The result suggests that PAB may mainly affect HIF1α post-transcriptional events and that reduction of VEGF secretion from the PAB-treated hypoxic tumor cells is attributable to the down-regulation of HIF-1α–mediated VEGF mRNA transcription.

To validate whether PAB mainly affects HIF-1α at post-transcriptional events, we investigated the impact of PI3K and MAPK pathways on HIF-1α protein level in hypoxic MDA-MB-468 cells. It has been demonstrated that the PI3K signaling is involved in the stabilization of HIF-1α, whereas the MAPK pathway stimulates HIF-1 transcriptional activity without affecting HIF-1α protein expression (13, 14). In this study, we con-

[4] Unpublished observations.

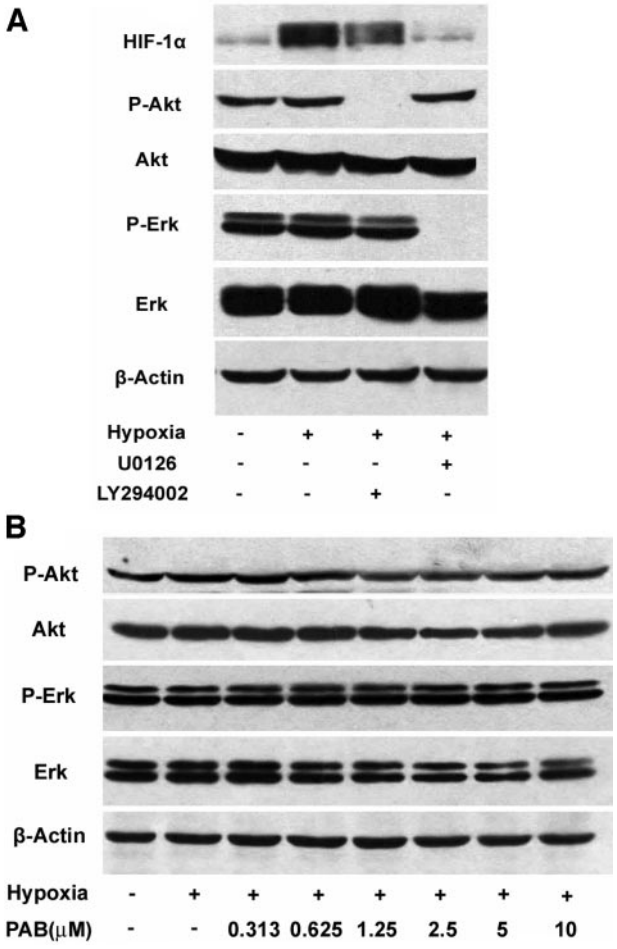


*Fig. 9* Effect of PAB on PI3K and p42/p44 MAPK pathways in MDA-MB-468 cells. *A,* effect of PI3K and MEK inhibitors on hypoxia-induced HIF-1α expression. Cells were treated with 50 μmol/L LY294002 or 100 μmol/L U0126 under hypoxia for 16 hours before an HIF-1α immunoblot assay. *B,* effect of PAB on the phosphorylation of Akt and Erk. Cells were treated with different concentrations of PAB under hypoxia for 16 hours before the corresponding immunoblot assay. Data shown are representative of three independent experiments.

firmed the role of the PI3K signaling, and we found that the MAPK pathway was also involved in the expression of HIF-1α protein in hypoxic MDA-MB-468 cells (Fig. 9*A*). This difference may be ascribed to the different cell models used between these experiments, which indicates the specificity of tumor type for HIF signaling modulation. Unexpectedly, PAB did not affect either PI3K or MAPK pathways (Fig. 9*B*), so we additionally tested the proteasome pathway and revealed that PAB accelerated HIF-1α protein degradation via this pathway. The stability of HIF-1α protein is regulated by oxygen tension. Under hypoxia, HIF-1α is not hydroxylated by specific HIF-prolyl hydroxylases, which prevents its interaction with pVHL and its subsequent ubiquitination and degradation, and, therefore, maintains its stability (29, 33, 34). PAB completely reversed the hypoxia-induced rise of HIF-1α protein in MDA-MB-468 cells. MG-132, the selective proteasome inhibitor rescued the PAB-mediated decrease of HIF-1α protein (Fig. 10). Nevertheless, the MG-132–raised HIF-1α protein lacked transcriptional activity because of a lack of change at the level of VEGF mRNA in the same cells (data not shown). The reason may be that the proteasome inhibitor MG-132 alters the nuclear-cytoplasm distribution and/or conformation of the HIF-1α protein (30). In the consideration of a lack of change in HIF-1α mRNA level and phosphorylated Akt and Erk levels in the PAB-treated hypoxic MDA-MB-468 cells, the enhanced degradation activity of the proteasome pathway appears to play a principal role in the PAB-induced reduction of HIF-1α protein.

Taking these results together, we demonstrate that PAB possesses dual roles, the direct action on endothelial cells and reduction of the VEGF paracrine secretion from tumor cells. The dual activities are interesting because few compounds, until now, possess the same effects. The known angiogenesis inhibitors could be classified into three classes. The first class is the agents blocking growth-factor activity, including VEGF signaling, such as the monoclonal antibody Avastin (35) and the VEGF receptor tyrosine kinase inhibitor SU5416 (36). The second class is the compounds inhibiting the matrix metalloproteinases responsible for breaking up the extracellular matrix and allowing endothelial cells to invade into it, *e.g.,* Marimastat, AG3340, and Bay 12–9566 (37). The third class is the agents targeting and inhibiting endothelial cells directly, including many endogenous angiogenesis inhibitors such as angiostatin (38) and endostatin (39). All of them arrested tumor growth in preclinical studies, but, unfortunately, most of them failed in human trials. No angiogenesis inhibitor used alone in clinical phase has been approved thus far. Thus, recently, combinations of several angiogenesis inhibitors have been recommended for treatment of human cancer, because they may interfere with angiogenesis at different levels. In this study, the compound PAB has been revealed to not only exert its antiangiogenic activities directly targeting endothelial cells, but also to inhibit the production of the angiogenic factor VEGF regulated by HIF-1 in hypoxic tumor cells. Such dual activities of PAB, different from the relatively single effects of other angiogenesis inhibitors, can be reasonably inferred to allow better *in vivo* and even better clinical effects as a novel angiogenesis inhibitor.

PAB acceleration in HIF-1α protein degradation by stimulating the proteasome pathway is also highly worth noting. To date, reduction of protein levels by compounds has been re-

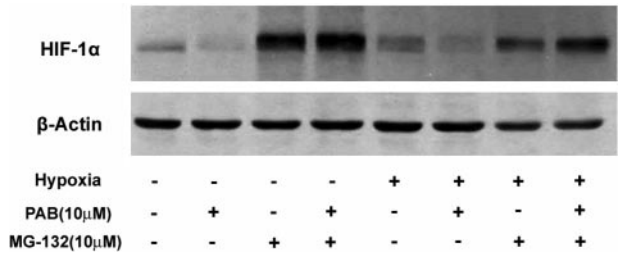


*Fig. 10* Effect of PAB on the proteasome pathway in MDA-MB-468 cells. Cells were treated with 0.1% DMSO, 10 μmol/L PAB, and 10 μmol/L MG-132 plus 10 μmol/L PAB for 16 hours under normoxia or hypoxia, respectively. Then, the cells were lysed and analyzed by Western blotting with antibodies against HIF-1α and β-actin. Data shown are representative of three independent experiments.

ported to result mainly from down-regulation of the corresponding gene expression, and, rarely, if ever, from speedup of proteasome-mediated protein breakdown. Additional investigation on this action of PAB, especially on its molecular mechanism of stimulating the proteasome pathway, may well generate new therapeutic opportunities.

In summary, our study reveals that PAB displays the dual activities of directly inhibiting endothelial cells as well as abrogating paracrine stimulation of VEGF from tumor cells. Additionally, PAB accelerates HIF-1α protein degradation most likely by stimulating the proteasome pathway in MDA-MB-468 cells. Additional studies will focus on evaluating its antiangiogenic effect in human tumor xenograft models in nude mice and dissecting the molecular mechanism of its action on the proteasome pathway.

## REFERENCES

1. Folkman J. What is the evidence that tumors are angiogenesis dependent? J. Natl Cancer Inst 1990;82:4–6.

2. Hanahan D, Folkman J. Patterns and emerging mechanisms of the angiogenic switch during tumorigenesis. Cell 1996;86:353–64.

3. Zetter BR. Angiogenesis and tumor metastasis. Annu Rev Med 1998;49:407–24.

4. Translational Research: the Role of VEGF in Tumor Angiogenesis. Proceedings of a symposium. Washington, DC, USA. November 16, 1999. Oncologist 2000; 5 Suppl 1: S1–57.

5. Carmeliet P, Ferreira V, Breier G, et al. Abnormal blood vessel development and lethality in embryos lacking a single VEGF allele. Nature (Lond) 1996;380:435–9.

6. Risau W. Mechanisms of angiogenesis. Nature (Lond) 1997;386: 671–4.

7. Minchenko A, Bauer T, Salceda S, Caro J. Hypoxic stimulation of vascular endothelial growth factor expression in vitro and in vivo. Lab Investig 1994;71:374–9.

8. Shweiki D, Itin A, Soffer D, Keshet E. Vascular endothelial growth factor induced by hypoxia may mediate hypoxia-initiated angiogenesis. Nature (Lond) 1992;359:843–5.

9. Forsythe JA, Jiang BH, Iyer NV, et al. Activation of vascular endothelial growth factor gene transcription by hypoxia-inducible factor 1. Mol Cell Biol 1996;16:4604–13.

10. Wang GL, Semenza GL. Purification and characterization of hypoxia-inducible factor 1. J Biol Chem 1995;270:1230–7.

11. Semenza GL. Hypoxia-inducible factor 1: oxygen homeostasis and disease pathophysiology. Trends Mol Med 2001;7:345–50.

12. Semenza GL, Jiang BH, Leung SW, et al. Hypoxia response elements in the aldolase A, enolase 1, and lactate dehydrogenase A gene promoters contain essential binding sites for hypoxia-inducible factor 1. J Biol Chem 1996;271:32529–37.

13. Jiang BH, Jiang G, Zheng JZ, Lu Z, Hunter T, Vogt PK. Phosphatidylinositol 3-kinase signaling controls levels of hypoxia-inducible factor 1. Cell Growth Differ 2001;12:363–9.

14. Hur E, Chang KY, Lee E, Lee SK, Park H. Mitogen-activated protein kinase kinase inhibitor PD98059 blocks the trans-activation but not the stabilization or DNA binding ability of hypoxia-inducible factor-1alpha. Mol Pharmacol 2001;59:1216–24.

15. Zhong H, De Marzo AM, Laughner E, et al. Overexpression of hypoxia-inducible factor 1alpha in common human cancers and their metastases. Cancer Res 1999;59:5830–5.

16. Ryan HE, Lo J, Johnson RS. HIF-1 alpha is required for solid tumor formation and embryonic vascularization. EMBO J 1998;17:3005–15.

17. Bos R, Zhong H, Hanrahan CF, et al. Levels of hypoxia-inducible factor-1 alpha during breast carcinogenesis. J Natl Cancer Inst 2001;93: 309–14.

18. Yang SP, Dong L, Wang Y, Wu Y, Yue JM. Antifungal diterpenoids of Pseudolarix kaempferi, and their structure-activity relationship study. Bioorg Med Chem 2003;11:4577–84.

19. Xiao D, Tan W, Li M, Ding J. Antiangiogenic potential of 10-hydroxycamptothecin. Life Sci 2001;69:1619–28.

20. Koyama S, Takagi H, Otani A, Suzuma K, Nishimura K, Honda Y. Tranilast inhibits protein kinase C-dependent signalling pathway linked to angiogenic activities and gene expression of retinal microcapillary endothelial cells. Br J Pharmacol 1999;127:537–45.

21. Sheu JR, Fu CC, Tsai ML, Chung WJ. Effect of U-995, a potent shark cartilage-derived angiogenesis inhibitor, on anti-angiogenesis and anti-tumor activities. Anticancer Res 18:4435–41, 1998.

22. Ashton AW, Yokota R, John G, et al. Inhibition of endothelial cell migration, intercellular communication, and vascular tube formation by thromboxane A(2). J Biol Chem 1999;274:35562–70.

23. Tan WF, Lin LP, Li MH, et al. Quercetin, a dietary-derived flavonoid, possesses antiangiogenic potential. Eur Pharmacol. 459:255–62, 2003.

24. Blancher C, Moore JW, Talks KL, Houlbrook S, Harris AL. Relationship of hypoxia-inducible factor (HIF)-1alpha and HIF-2alpha expression to vascular endothelial growth factor induction and hypoxia survival in human breast cancer cell lines. Cancer Res 2000;60: 7106–13.

25. Rossler J, Breit S, Havers W, Schweigerer L. Vascular endothelial growth factor expression in human neuroblastoma: up-regulation by hypoxia. Int J Cancer 1999;81:113–7.

26. Chun YS, Yeo EJ, Choi E, et al. Inhibitory effect of YC-1 on the hypoxic induction of erythropoietin and vascular endothelial growth factor in Hep3B cells. Biochem Pharmacol 2001;61:947–54.

27. Miao ZH, Ding J. Transcription factor c-Jun activation represses mdr-1 gene expression. Cancer Res 2003;63:4527–32.

28. Pan DJ, Li ZL, Hu CQ, Chen K, Chang JJ, Lee KH. The cytotoxic principles of Pseudolarix kaempferi: pseudolaric acid-A and -B and related derivatives. Planta Med 1990;56:383–5.

29. Ilan N, Mahooti S, Madri JA. Distinct signal transduction pathways are utilized during the tube formation and survival phases of in vitro angiogenesis. J Cell Sci 1998;111:3621–31.

30. Huang LE, Gu J, Schau M, Bunn HF. Regulation of hypoxia-inducible factor 1alpha is mediated by an O2-dependent degradation domain via the ubiquitin-proteasome pathway. Proc Natl Acad Sci USA 1998;95:7987–92.

31. Mabjeesh NJ, Escuin D, LaVallee TM, et al. 2ME2 inhibits tumor growth and angiogenesis by disrupting microtubules and dysregulating HIF. Cancer Cell 2003;3:363–75.

32. Wang WC, Lu RF, Zhao SX, Gu ZP. Comparison of early pregnancy-terminating effect and toxicity between pseudolaric acids A and B. Zhongguo Yao Li Xue Bao 1988;9:445–8.

33. Kallio PJ, Wilson WJ, O'Brien S, Makino Y, Poellinger L. Regulation of the hypoxia-inducible transcription factor 1alpha by the ubiquitin-proteasome pathway. J Biol Chem 1999;274:6519–25.

34. Bruick RK, McKnight SL. A conserved family of prolyl-4-hydroxylases that modify HIF. Science (Wash DC) 2001;294:1337–40.

35. Bevacizumab. Anti-VEGF monoclonal antibody, avastin, rhumab-VEGF. Drugs R D. 2002;3:28–30.

36. Vajkoczy P, Menger MD, Vollmar B, et al. Inhibition of tumor growth, angiogenesis, and microcirculation by the novel Flk-1 inhibitor SU5416 as assessed by intravital multi-fluorescence videomicroscopy. Neoplasia 1999;1:31–41.

37. Klohs WD, Hamby JM. Antiangiogenic agents. Curr Opin Biotechnol 1999;10:544–9.

38. Cao Y, Ji RW, Davidson D, et al. Kringle domains of human angiostatin. Characterization of the anti-proliferative activity on endothelial cells. J Biol Chem 1996;271:29461–7.

39. Yamaguchi N, Anand-Apte B, Lee M, et al. Endostatin inhibits VEGF-induced endothelial cell migration and tumor growth independently of zinc binding. EMBO J 1999;18:4414–23.